(Received 17 March 2025, Accepted 14 May 2025, Scheduled 29 May 2025)

FDTD Modeling of Lightning Electromagnetic Fields over Mixed and Sloped Domains Using Staircase Approximation

Mohamed Omari*, Abdenbi Mimouni, and Imane Ghlib

Laboratory of Electrical Engineering and Plasmas, University of Tiaret, Tiaret 14000, Algeria

ABSTRACT: This paper investigates the modeling of lightning electromagnetic (EM) fields over mixed propagation paths, including land-ocean and land-lake interfaces with slope angles, using Finite-Difference Time-Domain (FDTD) method combined with staircase approximation. Two scenarios are considered: a land strike involving a soil-ocean domain and a real-world lightning strike to the CN Tower with a land-Lake Ontario interface. The return stroke currents are modeled using established MTLE model, and electromagnetic fields are computed above and below ground. Simulation results demonstrate strong agreement with previously published Finite Element Method (FEM) results, confirming the accuracy of the proposed approach. The study highlights the significant impact of slope angles on electromagnetic field components, particularly underground fields near mixed interfaces, and confirms the effectiveness of the staircase approximation for modeling sloped geometries in FDTD. These findings contribute to improving the assessment of lightning effects in complex environments, including urban areas and mixed land-water regions.

1. INTRODUCTION

The electromagnetic radiation emitted by lightning poses a significant threat to both electrical and communication systems [1–3]. Understanding and characterizing the electromagnetic fields generated by lightning enables more effective protection for sensitive systems [4]. FDTD method has emerged as a highly recommended and extensively used approach in electromagnetic field simulations. Since the seminal work of Yee (1966), which demonstrates that Maxwell's equations can be replaced by a set of finite difference equations [5], this method has been distinguished by its robustness and flexibility [6]. Moreover, its ease of implementation in computer codes [7, 8] makes it a favored option [9] among researchers and practitioners alike. Numerous studies were conducted on the computation of electromagnetic fields in the vicinity of a lightning discharge using FDTD. Yang and Zhou [10] introduced two methods: the quasi-image formula and the FDTD method for low ground conductivity. The latter was employed as a benchmark to assess the validity of the Cooray-Rubinstein formula [11, 12]. Mimouni et al. [13, 14] conducted an analysis of the electromagnetic environment in close proximity to lightning return strokes to the ground and tall towers, respectively. They used FDTD method along with engineering models for their investigations.

To model arbitrary geometries that deviate from a Cartesian grid, staircase approximation emerged as the most straightforward and widely adopted approach [15, 16]. Furthermore, this approximation was used to validate the reliability and effectiveness of alternative methods [17]. Numerous studies tackled the challenge of staircasing errors [18–20]. Schneider and Shlager [15] discovered that errors associated with staircase approximation were negligible when the diagonal of the staircase (representing the hypotenuse of the triangle formed by the stairsteps) was smaller than half a wavelength at the highest frequency.

Numerous studies were conducted on vertically stratified ground. Shoory et al. [21] provided a review of simplified analytical expressions derived by Wait [22], employing the concept of attenuation function to assess lightning electromagnetic fields over vertically stratified ground. Paknahad et al. [23] analyzed the impact of the slope angle on lightning electromagnetic fields along mixed land-ocean propagation paths, employing the Comsol Multiphysics software, which was based on the finite element method for solving Maxwell's equations. Recently, Li et al. [24] analyzed the impact of lossy ground on lightning-generated electric field characteristics, using simultaneous measurements of lightning currents and radiated fields at different distances from rocket-triggered lightning. Then, in [25], Li et al. examined the lightning electromagnetic fields, incorporating the horizontal stratification of the soil and the frequency-dependent behavior of its electrical parameters. Both forms of lightning current, typical first and subsequent return strokes, were used in the analysis.

Hou et al. [26] investigated the impact of high mountains on the propagation of lightning electromagnetic fields using 2-D FDTD simulations. Their study considered factors such as ground conductivity, mountain height and width, as well as its position within the propagation domain, on the electromagnetic fields. In [27], Mestriner and Nicora conducted a simulation depicting the electromagnetic radiation resulting from a lightning strike over the sea, while considering the presence of a slope angle between the sea and the ground, as well as the elevation of the ground relative to sea level. This was achieved using

* Corresponding author: Mohamed Omari (mohamed.omari@univ-tiaret.dz).

the FEM method within the COMSOL Multiphysics software. In a more recent study, Jiang et al. [28] employed a simulation geometry incorporating three layers of ground to explore the characteristics of lightning electromagnetic fields. They investigated various simulation scenarios involving the manipulation of electrical parameters across the layers and implemented the perfectly matched layer absorbing boundary condition to confine the simulation space.

Tall towers have been used for lightning current measurements and are among the most common structures exposed to lightning [29–32]. This preference arose from their high prospects of lightning strikes, prompting researchers to heavily invest in equipping these structures with an array of instruments. These instruments were designed for measuring both electromagnetic fields and electrical current pertaining to lightning and were strategically placed at various heights along these towers [33, 34]. Consequently, the lightning return stroke current initiated to a tall object and its associated electromagnetic fields were different from those produced by lightning initiated to flat ground [35]. As a result, Heidler and Paul [36] examined the phenomenon of field enhancement during lightning strikes on the Peissenberg Tower in Germany. Typically, between 10 and 30 km, the field enhancement could surpass 100%. However, this enhancement notably diminished with a reduction in soil conductivity (σ) and an increase in distance. Li et al. [37] introduced an extended distributed circuit aimed at modeling the interaction between lightning channels and tall structures. This approach incorporated the dynamic attributes of the corona sheath while considering the nonlinear, nonuniform, and time-evolving characteristics inherent in lightning channels. Subsequently, this model was employed to simulate lightning surges occurring in wind turbine systems.

Few studies were available regarding the interaction of lightning with high objects in the presence of stratified ground or even a mixed propagation domain. Omari and Mimouni [38, 39], using the FDTD method, examined how horizontal ground stratification influenced electromagnetic fields both in close proximity and at distant locations from the Peissenberg Tower subjected to lightning strikes.

The aim of this paper is to integrate staircase approximation into the 2-D FDTD method to compute the lightning electromagnetic fields within a mixed two-layer propagation domain consisting of soil and ocean, with a slope angle in between. To get as close as possible to reality, the work is extended to a real-world scenario involving lightning striking the CN Tower to study the effect of this slope angle of the interface land-Ontario Lake on the electromagnetic fields.

The structure of this paper is as follows. Section 2 presents a concise overview of the staircase approximation and the modeling of lightning electromagnetic fields using FDTD method. Section 3 details the validation of the proposed approach, presents the simulation results, and provides a comprehensive discussion. Finally, Section 4 concludes the paper with a summary of key findings and final remarks.

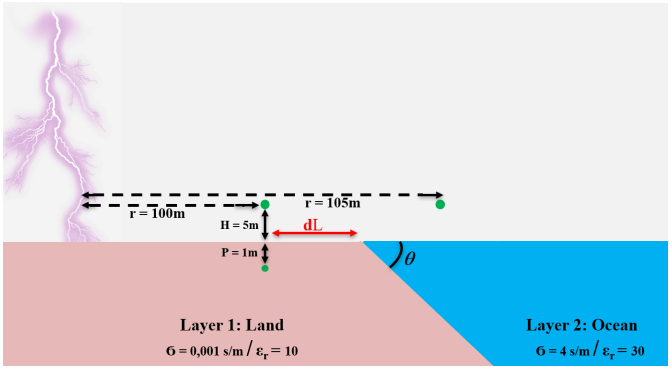

FIGURE 1. The problem geometry corresponding to land strike.

2. THE ADOPTED APPROACH AND THE COMPUTATIONAL MODELS

2.1. The FDTD Method and the Staircase Approach

Since FDTD method operates with a square mesh, staircase approximation becomes necessary for modeling the interface between the ground and ocean. Figs. 1 and 2 illustrate geometries of the respective scenarios, showcasing the various parameters involved in lightning strikes initiated in the soil and ocean, respectively.

Figure 1 depicts the geometry utilized in the simulation, featuring a horizontal distance of $R = 2$ km, an underground depth of 100 m, and a lightning channel height of $H = 3$ km. The spatial steps, both horizontally and vertically, are set at $\Delta r = \Delta z = 1$ m, while the time step $\Delta t = 1$ ns is chosen in accordance with the stability condition of the FDTD method [38, 39].

Our calculation code is developed in Fortran PowerStation and incorporates vertical stratification by using a straightforward formula $R_l = f(\theta^\circ)$ to determine $\mathbf{R_l}$ for each vertical space step j.

$$R_{\mathbf{L}} = \frac{[R_{\mathbf{Lsurf}} \times (\tan(\theta_{rad}))] + [D_{\min} - (j-1) \times \Delta z] - \Delta r}{\tan(\theta_{rad}) \times \Delta r} \quad (1)$$

$$D_{\min} = abs(z_{\min}/\Delta z) \quad (2)$$

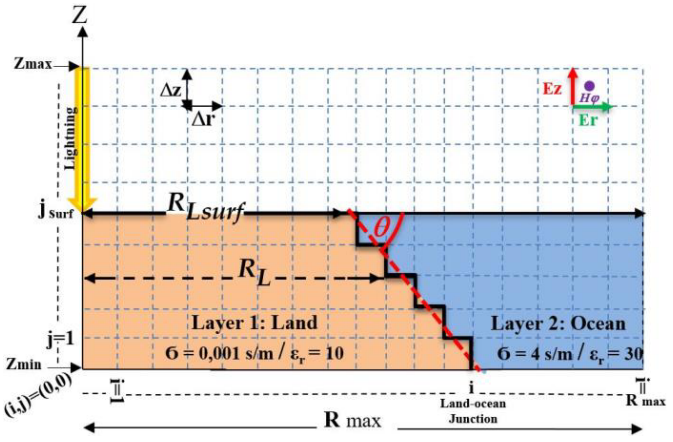

FIGURE 2. FDTD mesh representation of the land-ocean problem geometry.

$$\theta_{rad} = (\theta^\circ \times \pi)/180 \tag{3}$$

When the radial distance $r = i \times \Delta r$ is less than R_L (see Fig. 2) the code employs the electrical parameters of the ground to calculate electromagnetic radiations. Conversely, when r exceeds R_L, the code switches to the electrical parameters of the second layer (ocean). In the simulation, the air is assumed to be lossless ($\sigma = 0$ S/m, $\varepsilon_r = 1$), while the land and ocean are characterized by finite electrical conductivity ($\sigma_{\text{land}} = 0.001$ S/m, $\varepsilon_{r\text{land}} = 10$) and ($\sigma_{\text{ocean}} = 4$ S/m, $\varepsilon_{r\text{ocean}} = 30$) [23].

The electromagnetic fields produced by lightning are calculated through the direct solution of Maxwell's differential equations using FDTD method and Yee discretization scheme, implemented in two-dimensional (2D) cylindrical coordinates.

$$\frac{\partial H_\varphi}{\partial_t} = \frac{1}{\mu}\left[\frac{\partial E_e}{\partial_r} - \frac{\partial E_r}{\partial_Z}\right] \tag{4}$$

$$\partial E_r + \varepsilon\frac{\partial E_z}{\partial_t} = -\frac{\partial H_\varphi}{d_z} \tag{5}$$

$$\partial E_z + \varepsilon\frac{\partial E_r}{\partial_t} = -\frac{1}{r}\frac{\partial(rH_\varphi)}{\partial_r} \tag{6}$$

To solve these equations numerically using FDTD, we approximate derivatives using finite differences. Electric field components E_r, E_z and azimuthal magnetic field H_φ can be determined as outlined in [38, 39]:

$$E_z^{n+1}(i, j+1/2) = \frac{2\varepsilon - \sigma\Delta t}{2\varepsilon + \Delta t}E_z^n\left(i, j+\frac{1}{2}\right) + \frac{2\Delta t}{(2\varepsilon+\sigma\Delta t)\, ri\Delta r}\left[\begin{matrix} r_{i+(\frac{1}{2})}H_\varphi^{n+\frac{1}{2}}\left(i+\frac{1}{2}, j+\frac{1}{2}\right) \\ -r_{i-(\frac{1}{2})}H_\varphi^{n+\frac{1}{2}}\left(i-\frac{1}{2}, j+\frac{1}{2}\right)\end{matrix}\right] \tag{7}$$

$$E_r^{n+1}(i+1/2, j) = \frac{2\varepsilon - \sigma\Delta t}{2\varepsilon + \Delta t}E_r^n\left(i+\frac{1}{2}, j\right) - \frac{2\Delta t}{(2\varepsilon+\sigma\Delta t)\,\Delta r}\left[\begin{matrix} H_\varphi^{n+\frac{1}{2}}\left(i+\frac{1}{2}, j+\frac{1}{2}\right) \\ -H_\varphi^{n+\frac{1}{2}}\left(i+\frac{1}{2}, j-\frac{1}{2}\right)\end{matrix}\right] \tag{8}$$

$$H_\varphi^{n+\frac{1}{2}}\left(i+\frac{1}{2}, j+\frac{1}{2}\right) = H_\varphi^{n-\frac{1}{2}}\left(i+\frac{1}{2}, j+\frac{1}{2}\right) + \frac{\Delta t}{\mu\Delta r}\left[E_z^n\left(i+1, j+\frac{1}{2}\right) - E_z^n\left(i, j+\frac{1}{2}\right)\right] - \frac{\Delta t}{\mu\Delta z}\left[E_r^n\left(i+\frac{1}{2}, j+1\right) - E_r^n\left(i+\frac{1}{2}, j\right)\right] \tag{9}$$

2.2. Absorbing Boundary Conditions

Usually, simulating electromagnetic fields generated by lightning typically involves transforming the infinite real domain into a computationally finite domain. In this paper, we utilize first-order *Mur* absorbing boundary conditions (ABCs) [40] at the artificial boundaries of the chosen geometry.

2.3. The Distribution of the Current along the Lightning Channel

In this study, the subsequent return stroke at the channel base is represented using the sum of two *Heidler*'s functions [41], as expressed below:

$$i_0(h,t) = \frac{I_{01}}{\eta_1}\frac{(t/\tau_{11})^2}{1+(t/\tau_{11})^2}e^{(-t/\tau_{21})} + \frac{I_{02}}{\eta_2}\frac{(t/\tau_{12})^2}{1+(t/\tau_{12})^2}e^{(-t/\tau_{22})} \tag{10}$$

The distribution of the current along the lightning channel is represented by adopting the Modified Transmission Line with Exponential decay "MTLE" model [43, 44], with $\lambda = 2$ km, which allows describing the current distribution as a function of the current at the base of the channel and the speed of the return stroke.

The first return stroke current (see Fig. 3) is defined by a peak amplitude of 29.5 kA and a maximum rate of rise of 12 kA/µs. In contrast, the subsequent return stroke current exhibits a lower peak amplitude of 12 kA but a steeper maximum rate of rise, reaching 40 kA/µs.

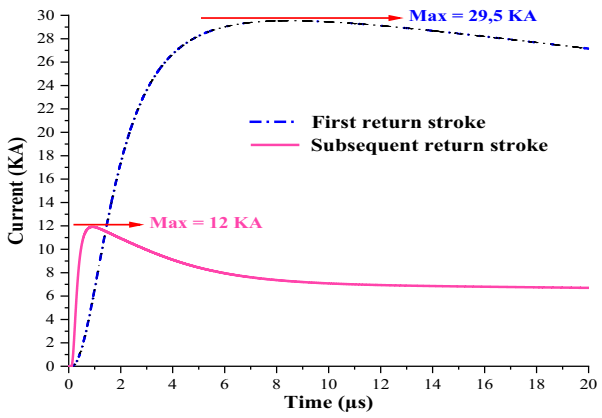

FIGURE 3. The channel base current.

3. SIMULATION RESULTS AND DISCUSSION

3.1. Land Strike

3.1.1. Validation of the Developed Code

Figures 4 and 5 illustrate the horizontal electric field generated by the subsequent return stroke current (as detailed in Table 1) at a horizontal distance of $r = 200$ m and a depth of $p = 1$ m, as well as at the ground surface. These calculations were performed at a distance of $dl = 1$ m from the land-ocean interface

TABLE 1. Parameters of the two Heidler's functions used to reproduce the channel-base current waveshape [42].

	I_{01}	τ_{11}	τ_{21}	N_1	I_{02}	τ_{12}	τ_{22}	N_2
First return stroke	28 (KA)	1.8 (µs)	95 (µs)	2	–			–
Subsequent return stroke	10.7 (KA)	0.25 (µs)	2.5 (µs)	2	6.5 (KA)	2 (µs)	230 (µs)	2

TABLE 2. Analyzing the diminishing influence of the slope angle at the Land-Ocean interface on lightning electromagnetic fields.

The used current		First return stroke						Subsequent return stroke					
Lightning EM field components		*Er*		*Ez*		*Hphi*		*Er*		*Ez*		*Hphi*	
The location of the observation point		Under the ground	Above the ground	Under the ground	Above the ground	Under the ground	Above the ground	Under the ground	Above the ground	Under the ground	Above the ground	Under the ground	Above the ground
The distance dL between the observation points and the junction land-ocean	dL = 1 m	+	+	+	-	+	-	+	+	+	-	+	-
	dL = 5 m	+	+	+	-	+	-	+	+	+	-	+	-
	dL = 10 m	+	+	+	-	-	-	+	+	+	-	+	-
	dL = 15 m	+	+	+	-	-	-	+	+	+	-	-	-
	dL = 20 m	+	+	+	-	-	-	-	+	+	-	-	-
	dL = 25 m	+	+	+	-	-	-	-	+	-	-	-	-
	dL = 30 m	+	+	+	-	-	-	-	+	-	-	-	-
	dL = 35 m	+	+	+	-	-	-	-	+	-	-	-	-
	dL = 40 m	+	-	+	-	-	-	-	-	-	-	-	-
	dL = 45 m	+	-	-	-	-	-	-	-	-	-	-	-
	dL = 50 m	+	-	-	-	-	-	-	-	-	-	-	-
	dL = 55 m	+	-	-	-	-	-	-	-	-	-	-	-
	dL = 60 m	-	-	-	-	-	-	-	-	-	-	-	-

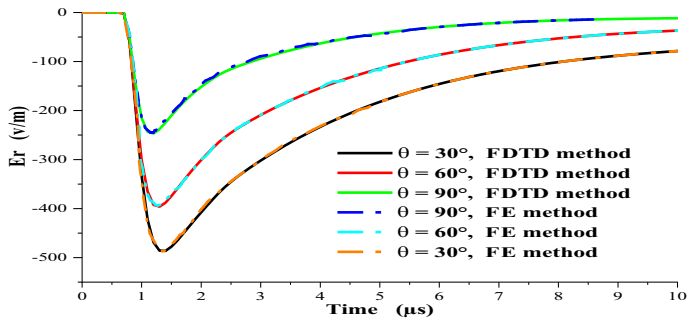

FIGURE 4. Horizontal electric field at depth of 1 m. $dL = 1$ m, FE method [23], FDTD method.

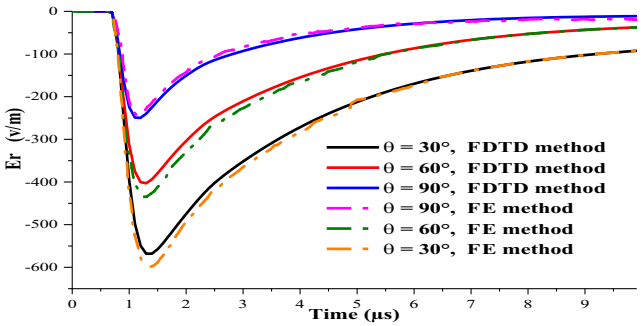

FIGURE 5. Horizontal electric field at the ground surface. $dL = 1$ m, FE method [23], FDTD method.

using FDTD method. The results are compared with those obtained using the FE method described in [23]. A strong agreement is observed between the results from the two methods, both below and above the ground surface.

This indicates that, given a wise selection of spatial steps, employing the staircase approximation within the FDTD method proves highly effective for modeling and simulating curved geometries or those featuring slope angles in electromagnetic applications.

The calculations were conducted for various values of dl (ranging from 1 m to 60 m in increments of 5 m) to pinpoint when the influence of the slope angle diminishes for each component of the electromagnetic field. The simulation results detailed in this section correspond to $dL = 1$ m. While not all results are shown, a summarized overview of the findings, along with an analysis, is provided (refer to Table 2). It is important to note that all results were obtained without accounting for the frequency-dependent properties of the soil, as the study focuses on evaluating electromagnetic fields at close distances. At such distances, it has been established that the electromagnetic fields generated by lightning are nearly unaffected by the soil's frequency-dependent characteristics [25].

3.1.2. Under-Ground Fields

Figures 6 and 7 present the horizontal electric field at $r = 100$ m and $r = 105$ m, respectively, from the lightning base channel, and depth of $p = 1$ m. For both observation points, the horizontal electric field generated by the first return stroke exhibits a higher amplitude and a significantly longer rise time than the field produced by the subsequent return stroke. These

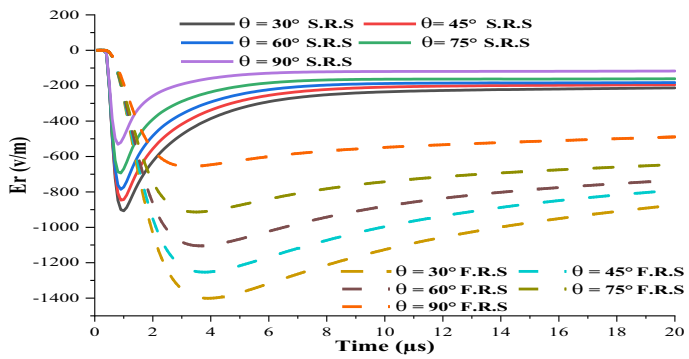

FIGURE 6. Horizontal electric field at $r = 100\,\text{m}$ for $dL = 1\,\text{m}$ and depth of $p = 1\,\text{m}$. (lines: subsequent return stroke S.R.S, dashed lines: first return stroke F.R.S).

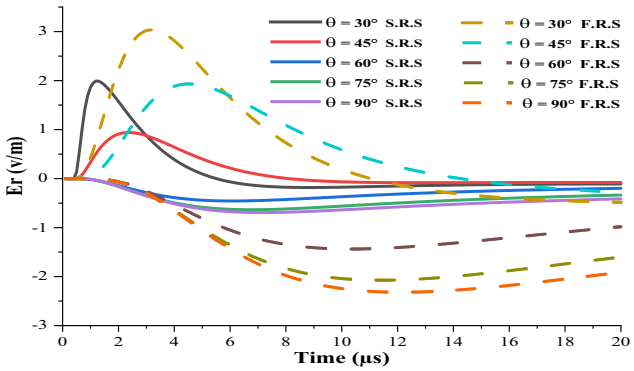

FIGURE 7. Horizontal electric field at $r = 105\,\text{m}$ and depth of $p = 1\,\text{m}$.

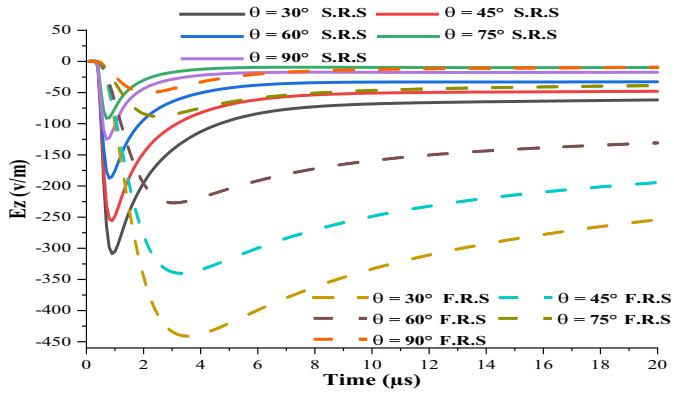

FIGURE 8. Vertical electric field at $r = 100\,\text{m}$ for $dL = 1\,\text{m}$ and depth of $p = 1\,\text{m}$.

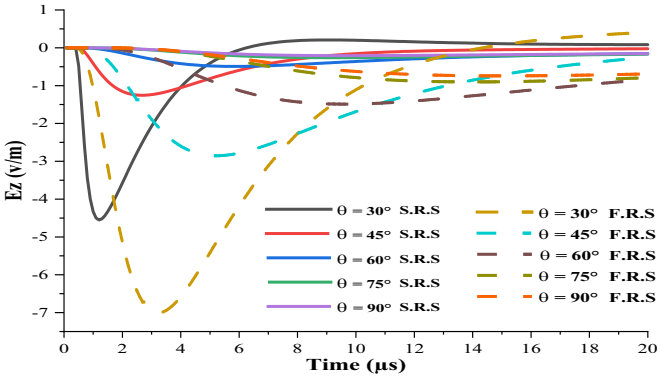

FIGURE 9. Vertical electric field at $r = 105\,\text{m}$ and depth of 1 m.

findings align with the characteristics observed in the current waveforms depicted in the graphs (Fig. 3). It can also be observed that this electric field component is affected by the slope angle in the vicinity of the land-ocean interface. Notably, this influence is more pronounced on the fields generated by the first return stroke. The horizontal electric field calculated below the ground surface (Fig. 6) exhibits a negative polarity, with its amplitude inversely proportional to the angle of inclination for both simulated current types (first return stroke and subsequent return stroke). In contrast, at the observation point inside the ocean (Fig. 7), the horizontal electric field displays a positive polarity for inclination angles of 30°and 45°. For higher angles (60°, 75°, and 90°), the horizontal electric field changes to a negative polarity.

Figures 8 and 9 present the vertical electric field at $r = 100\,\text{m}$ and $r = 105\,\text{m}$ from the lightning base channel, respectively, and at depth of $p = 1\,\text{m}$. It is noteworthy that the slope angle also affects the vertical component of the electric field, and this effect is more noticeable on graphs with the first return stroke than those generated by the subsequent return stroke. The variation of the angle has a greater effect on the vertical component than on the horizontal component of the electric field. From Fig. 8, it can be seen that the vertical electric field exhibits a negative polarity with an amplitude inversely proportional to the angle of inclination for both current types. When the subsequent return stroke current is used, the field also features a very rapid rise time. At $r = 105\,\text{m}$, inside the ocean (Fig. 9), the vertical electric field initially displays a negative polarity during the first few microseconds before transitioning to positive one. This polarity change is more pronounced when the first return stroke current is considered. In both cases, the amplitude remains inversely proportional to the slope angle, while the rise time is longer for the field generated by the first return stroke.

Figures 10 and 11 illustrate the azimuthal magnetic field at a distance of $r = 100\,\text{m}$ and $r = 105\,\text{m}$, respectively, and a depth of $p = 1\,\text{m}$. From Fig. 10, it appears that the slope angle does not affect the azimuthal magnetic field for the observation point located below the ground surface. In contrast when the observation point is located at a depth of 1 m inside the ocean (Fig. 11), a significant influence of the slope angle on the azimuthal component is observed, regardless of whether the first return stroke or the subsequent return stroke is used. As the angle increases, the amplitude of the azimuthal component consistently decreases. Additionally, the transition between the first return stroke and subsequent return stroke notably impacts both the amplitude and rise time of the azimuthal field.

3.1.3. Above the Ground Surface Fields

Figures 12 and 13 depict the horizontal electric field at a distance of $r = 100\,\text{m}$ ($dL = 1\,\text{m}$) and $r = 105\,\text{m}$, respec-

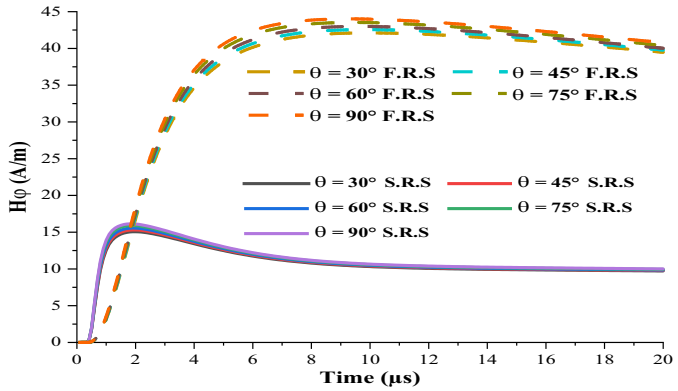

FIGURE 10. Azimuthal magnetic field at $r = 100\,\text{m}$, $p = 1\,\text{m}$, $dL = 1\,\text{m}$.

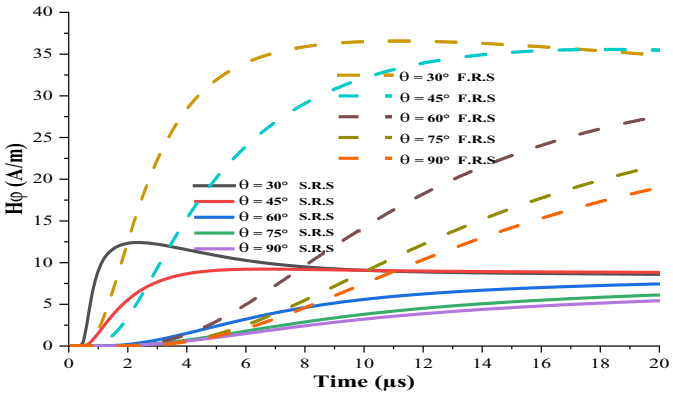

FIGURE 11. Azimuthal magnetic field at $r = 105\,\text{m}$ and depth of $p = 1\,\text{m}$.

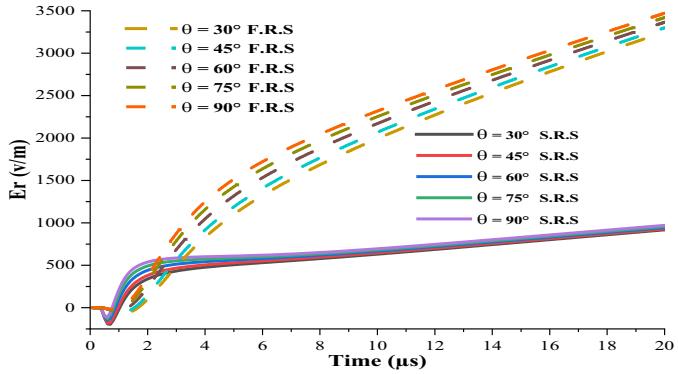

FIGURE 12. Horizontal electric field at $r = 100\,\text{m}$ and $H = 5\,\text{m}$. $dL = 1\,\text{m}$.

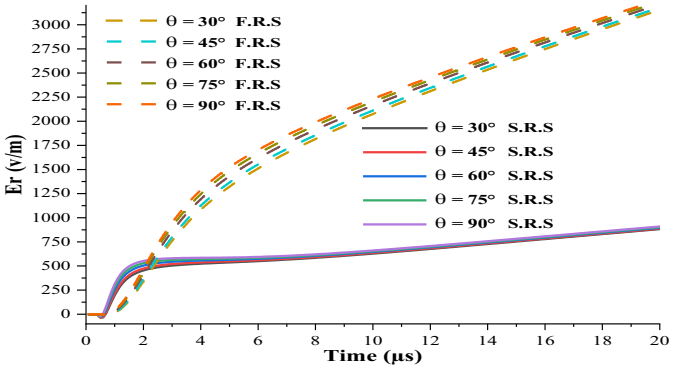

FIGURE 13. Horizontal electric field at $r = 105\,\text{m}$ and $H = 5\,\text{m}$.

tively, and with a height of 5 m above the ground using the first and subsequent return strokes. It is evident that above the ground, the magnitude of this component is greater than the underground scenario. The angle has a minor impact on the horizontal component above the ground at both observation points. For the subsequent return stroke, this effect is noticeable only during the early-time response and diminishes in the later stages. In contrast, for the first return stroke, the effect of the angle remains evident throughout the entire simulation time.

Figures 14 and 15 present, respectively, the above ground vertical electric field at a distance of $r = 100\,\text{m}$ ($dL = 1\,\text{m}$) and $r = 105\,\text{m}$ from the lightning base channel. It can be seen that the magnitude of the vertical component of the electric field is significantly greater than that of the same underground component at a depth of $p = 1\,\text{m}$. Unlike the underground case, the slope angle does not affect the vertical electric field above the ground surface, which is for both types of current (first and subsequent return strokes). Running the simulation with the parameters of either the first stroke or subsequent return stroke affects only the amplitude and rise time of the resulting fields.

Figures 16 and 17 present the above ground azimuthal magnetic field at $r = 100\,\text{m}$ ($dL = 1\,\text{m}$) and $r = 105\,\text{m}$ from lightning base channel, respectively. It is clear from these figures that the azimuthal magnetic field is easily determined using the approximation of a vertically stratified soil ($\theta = 90°$) whatever the value of the slope angle.

Table 2 provides an analysis to determine the exact distance dL at which the effect of the slope angle becomes negligible for all components of the lightning electromagnetic field. A "+" sign indicates the presence of the slope angle effect, while a "−" sign indicates that the effect has diminished to the point of being negligible.

An interesting approach for enhancing the robustness of simulation results in the presence of uncertainties and variability is the application of fuzzy similarity, as demonstrated in [45]. In the context of FDTD simulations, fuzzy similarity could allow for an effective and lightweight comparison between different simulated configurations or between simulation results and experimental data, explicitly accounting for the uncertain nature of the input conditions. Although the current study does not implement this method, it is recognized as a valuable tool for future model validation and for systematically addressing structural approximations and uncertain physical parameters in advanced numerical simulations.

Finite Element Method (FEM) is known to require considerably higher computational time for large-scale electromagnetic simulations, mainly due to the need for assembling and solving large sparse matrix systems, especially when fine meshing is employed. In contrast, the Finite-Difference Time-Domain (FDTD) method, based on an explicit time-stepping

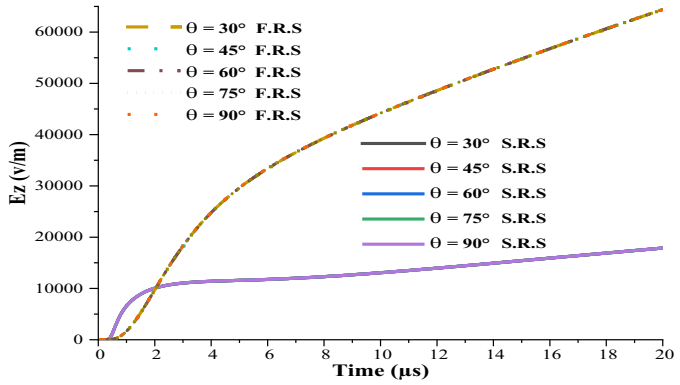

FIGURE 14. Vertical electric field at $H = 5\,\text{m}$ and $r = 100\,\text{m}$. $dL = 1\,\text{m}$.

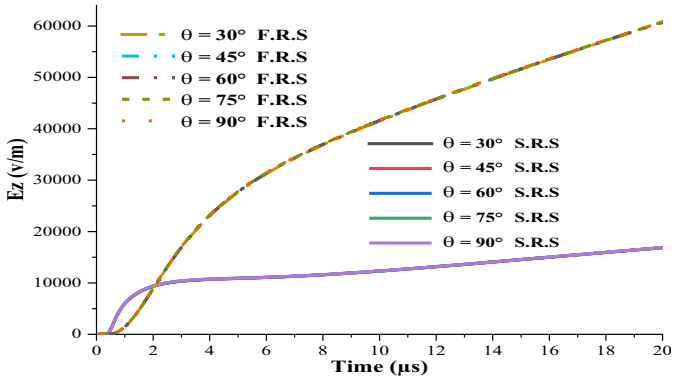

FIGURE 15. Vertical electric field at $H = 5\,\text{m}$ and $r = 105\,\text{m}$.

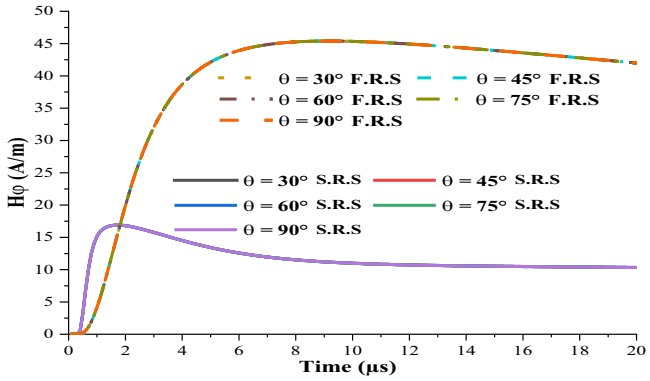

FIGURE 16. Azimuthal magnetic field at $r = 100\,\text{m}$. $dL = 1\,\text{m}$ and $H = 5\,\text{m}$.

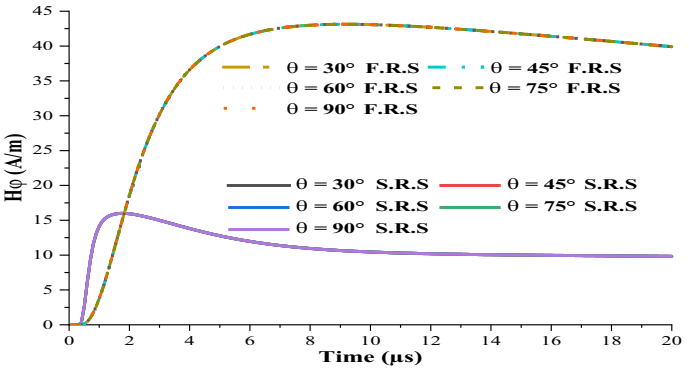

FIGURE 17. Azimuthal magnetic field at $r = 105\,\text{m}$ and $H = 5\,\text{m}$.

TABLE 3. Summary of FDTD vs. FEM computational characteristics.

Aspect	Finite-Difference Time-Domain (FDTD)	Finite Element Method (FEM)
Time-stepping	Explicit (fast updates)	Implicit (requires matrix solving)
CPU Time (per iteration)	Low (simple calculations at each point)	High (matrix assembly and inversion)
Total CPU Time (for large-scale simulations)	Lower (Efficient for large domains)	Higher (Computationally expensive for fine meshing)
Memory Usage	Low (Stores only field values at grid points)	High (Requires storing large sparse matrices)
Suitability for Large-Scale Domains	Excellent	Limited by computational cost
Flexibility for Complex small Geometries	Moderate	Excellent

scheme, achieves faster iteration speeds, lower memory usage, and greater overall computational efficiency for problems of this nature. Table 3, provides a comparative summary of the key characteristics of FDTD and FEM methods relevant to this study.

3.2. Practical Geometry Simulation (CN Tower Strike)

Building on the work presented in Part A and aiming to achieve greater alignment with real-world conditions, this second part focuses on analyzing the impact of the slope angle of the land-Ontario Lake interface on the electromagnetic fields generated by lightning strikes to the CN Tower in Toronto, Canada. The study employs staircase approximation and FDTD method, considering various inclination angles between the ground and Ontario Lake, as the precise value of this angle remains uncertain.

3.2.1. Distribution of Lightning Current along the Tower and the Lightning Channel

The model used to describe the lightning current distribution along the tower and lightning channel was proposed by Baba and Rakov [46]. This model is based on a lumped series voltage

source located at the junction point between the channel and striking object. Baba and Rakov demonstrated the equivalence of this representation to the distributed source model introduced by Rachidi et al. [47]. In their methodology, they provided a spatial-temporal distribution of the current along the channel and strike object, expressed in terms of the short-circuit current $i_{sc}(t)$:

For $0 \leq z' \leq h$

$$i(z',t) = \frac{1-\rho_t}{2} \sum_{n=0}^{\infty} \left[\begin{array}{c} \rho_t^n \rho_g^n i_{sc}\left(h, t - \frac{h-z'}{c} - \frac{2nh}{c}\right) \\ +\rho_g^{n+1} \rho_t^n i_{sc}\left(h, t - \frac{h+z'}{c} - \frac{2nh}{c}\right) \end{array} \right] \tag{11}$$

For $z' \geq h$

$$i(z',t) = \frac{1-\rho_t}{2} \left[\begin{array}{c} i_{sc}\left(h, t - \frac{z'-h}{v}\right) - \rho_t i_0\left(h, t - \frac{z'-h}{c}\right) \\ +\sum_{n=0}^{\infty} \rho_g^n \rho_t^{n-1}(1+\rho_t) i_{sc}(h, t - \frac{z'-h}{v} - \frac{2nh}{c}) \end{array} \right] \tag{12}$$

Variable h represents the tower's height, while ρ_t and ρ_g stand for the top and bottom current reflection coefficients concerning upward and downward propagation waves, respectively. c indicates the wave propagation speed along the strike object (the speed of light). Additionally, v signifies the return stroke front speed, whose chosen value, in this study, is 150 m/μs [48]. Lastly, n serves as an index denoting the successive multiple reflections taking place at two ends of the tower.

The short-circuit current, $i_{sc}(t)$, as depicted in the model by Baba and Rakov, corresponds to typical subsequent return strokes. It is represented by a combination of two Heidler's functions [41] with parameters including a peak value of 12 kA and a maximum steepness of 40 kA/μs. The specific parameters of the short-circuit current can be found in Table 1.

As seen in Fig. 18, the site chosen for this study is located in Toronto, Canada, hence the considered high object is the Canadian National Tower. The necessary tower parameters for the model developed by Baba and Rakov include its height ($h = 553$ m) and the reflection coefficients at the top and bottom, which have been set respectively, to specific values (-0.366 and 0.8) as provided by [46]. The electrical parameters of Ontario Lake are defined as follows: electrical conductivity $\sigma = 0.008$ S/m and relative permittivity $\varepsilon_r = 81$ [49]. The area surrounding the CN Tower is highly urbanized, with most structures constructed from materials such as clay brick, steel, or reinforced concrete, underlain by a water system. Estimating the equivalent ground conductivity in this area is challenging; however, it is likely to be somewhat lower than the conductivity associated with Ontario Lake [49] so estimated as $\sigma = 0.001$ S/m and relative permittivity $\varepsilon_r = 10$.

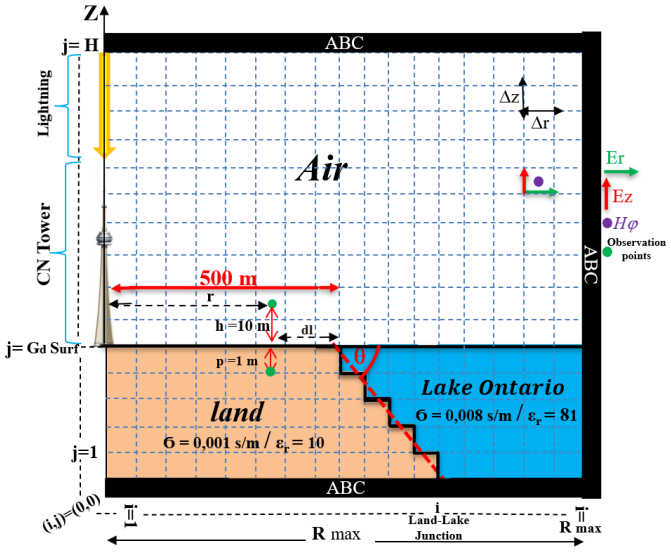

FIGURE 18. The adopted problem geometry.

The waveforms of the current assessed at both the top and base of the CN Tower are depicted in Fig. 19. The impact of multiple reflections at the tower's ends is readily apparent in these waveforms. Additionally, it is evident that the current at the tower's base exhibits a higher peak value, attributed to the positive reflected wave's contribution at ground level.

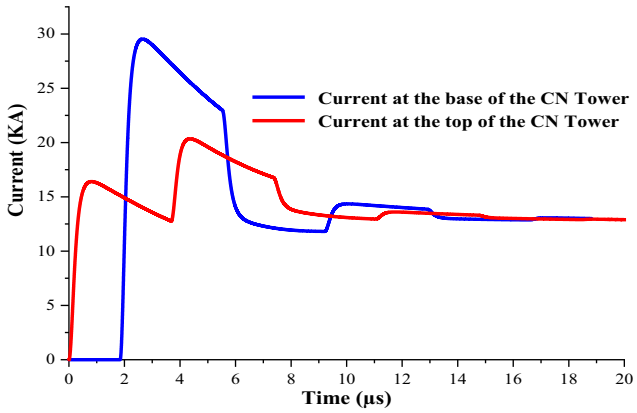

FIGURE 19. Lightning current at the base and at the top of the CN tower.

3.2.2. Validation of the Developed Code

To validate the computational code, the measured vertical electric field and azimuthal magnetic field at distances of 198 m and 185 m, respectively, from the Peissenberg tower, as published by Guerrieri et al. in 1996 [50] are used. The model of Rachidi et al. [47] is employed to represent the current distribution along both the lightning channel and Peissenberg tower, incorporating the MTLE model with a decay constant $\lambda = 1500$ m. The MTLE model is particularly suitable for these calculations, as it generates field predictions that closely approximate the available experimental data. It offers an optimal balance between mathematical simplicity and accuracy.

From Figs. 20 and 21, the simulated waveforms show strong agreement with the experimental results. The slight discrepancies observed between the measured and simulated electromagnetic fields can be attributed to various factors, including assumptions inherent in the theoretical models, experimental inaccuracies, the chosen values for reflection coefficients, and the estimated electrical parameters of the propagation domain used in the simulation.

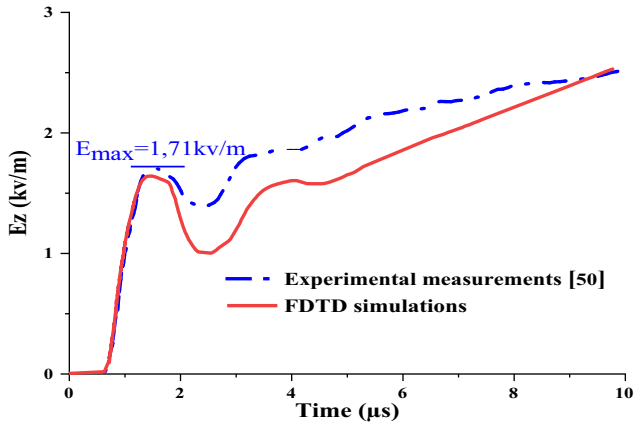

FIGURE 20. The vertical electric field simulated by FDTD and measured at 198 m from Peissenberg tower [50].

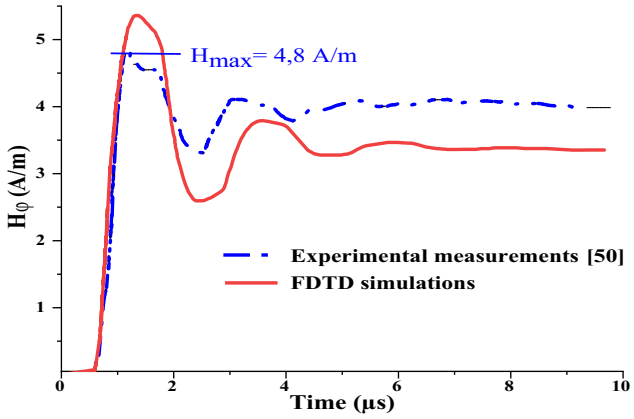

FIGURE 21. The azimuthal magnetic field simulated by FDTD and measured at 185 m from Peissenberg tower [50].

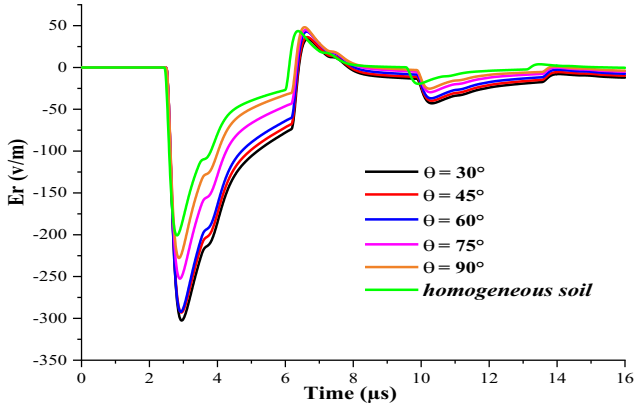

FIGURE 22. Horizontal electric field at $r = 499\,\text{m}$ ($dL = 1\,\text{m}$) and $p = 1\,\text{m}$.

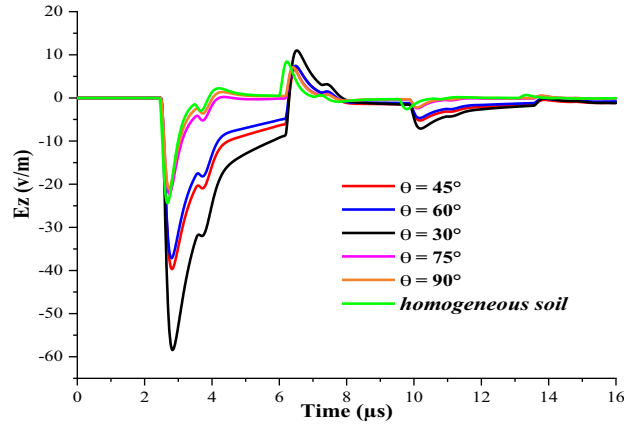

FIGURE 23. Vertical electric field at $r = 499\text{m}$ ($dL = 1\,\text{m}$) and $p = 1\,\text{m}$.

3.2.3. Underground Fields

The horizontal electric field generated by lightning strikes to the CN Tower is illustrated in Fig. 22. It can be seen that this electric field component is influenced by the slope angle of the land-lake interface. Similar to the observations of land strike, as the slope angle increases, the magnitude of this component decreases. The impact of the slope angle on the underground horizontal component, in the presence of a tower, appears less than the case when the lightning is initiated from a ground.

Furthermore, it is evident that the results differ when considering homogeneous ground as opposed to varying slope angles. Neglecting the presence of Lake Ontario leads to inaccuracies in electromagnetic fields predictions.

Figure 23 depicts the underground vertical electric field for a distance of $r = 499\,\text{m}$ ($dL = 1\,\text{m}$). It is evident that this underground component is significantly influenced by the slope angle. There is a notable discrepancy in peak values among different cases of slope angle variations, with the effects of multiple inversions of the current wave at the two ends of the tower becoming more pronounced. The peak values of the vertical electric field increase with the decrease of the slope angle value. Similar to the horizontal component, the vertical electric field is particularly affected by the slope angle in nearby regions ($dL = 1\,\text{m}$).

Moreover, the results of the vertical electric field in the presence of Lake Ontario differ from those obtained in the case of homogeneous ground without the lake. Achieving accuracy in the computation of lightning electromagnetic fields necessitates considering the propagation domain as close as possible to reality.

From Fig. 24 it appears that the azimuthal magnetic field, in the immediate vicinity of the land-lake junction, is not really influenced by the variation of the slope angle.

It can therefore be deduced that at distances equal to or greater than 1 m from the observation point to the meeting point between the two layers soil-lake, the azimuthal component of the electromagnetic field can be evaluated without taking into account the slope angle or the vertical stratification of the propagation domain. In other words, it can be calculated using only the electrical parameters of the first layer.

3.2.4. Above the Ground Surface Fields

From Fig. 25 illustrating the horizontal component of the electric field above the ground, it is evident that this component,

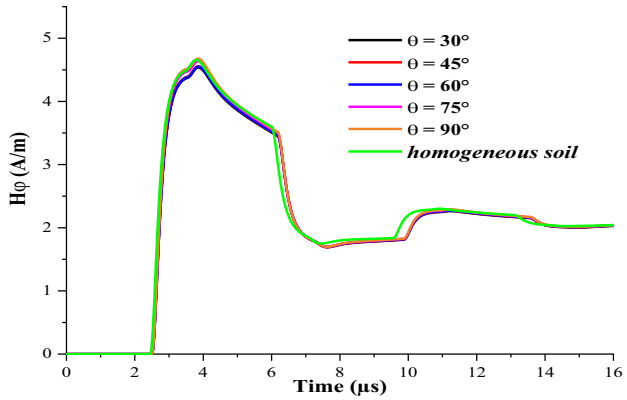

FIGURE 24. Azimuthal magnetic field at $r = 499\,\text{m}$ ($dL = 1\,\text{m}$) and $p = 1\,\text{m}$.

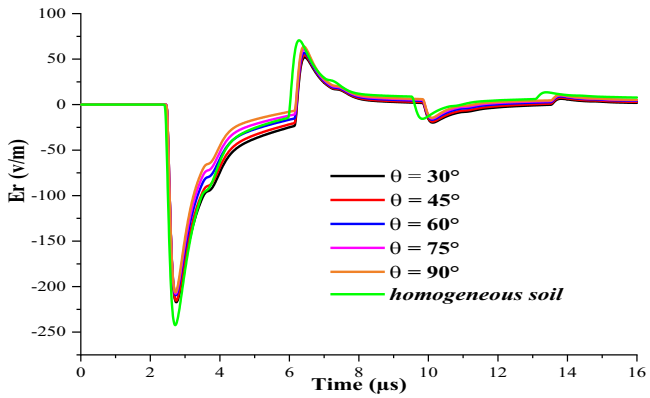

FIGURE 25. Horizontal electric field at $r = 499\,\text{m}$ ($dL = 1\,\text{m}$) and $H = 10\,\text{m}$.

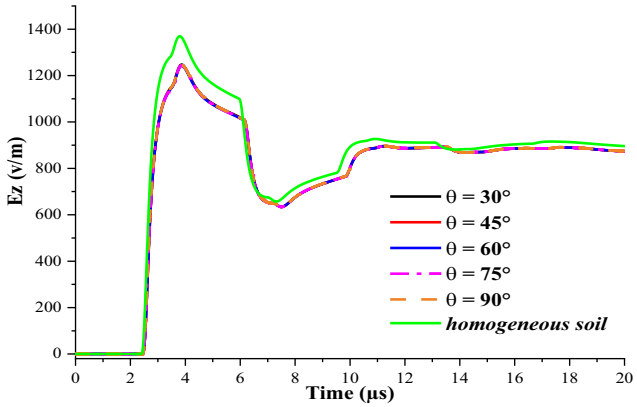

FIGURE 26. Vertical electric field at $r = 499\,\text{m}$ ($dL = 1\,\text{m}$) and $H = 10\,\text{m}$.

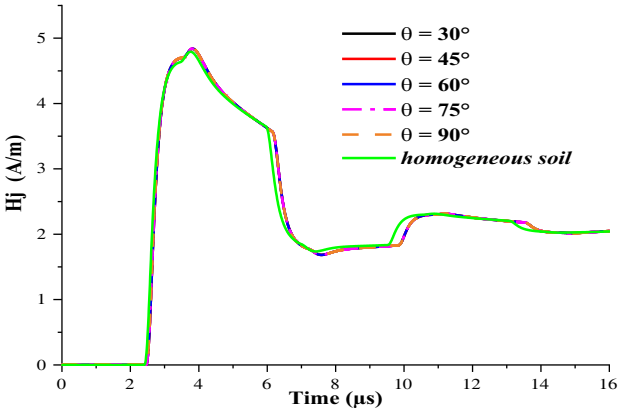

FIGURE 27. Azimuthal magnetic field at $r = 499\,\text{m}$ ($dL = 1\,\text{m}$) and $H = 10\,\text{m}$.

as in land strike scenario, is only minimally influenced by the slope angle of the land-lake interface. The magnitude of the horizontal component exhibits a decreasing trend as the angle of the land-ocean interface increases.

The vertical electric field (refer to Fig. 26) above ground remains unaffected by changes in the slope angle value, as the land case scenario. Regardless of whether the angle is set at $\theta = 30°$, $45°$, $60°$, $75°$, or $90°$, the results appear identical. However, similar to the horizontal electric field component, the vertical component is influenced by the presence of Lake Ontario. Compared to the case of homogeneous ground, the presence of the lake, with its higher electrical parameters than the soil, leads to a reduction in the magnitude of horizontal and vertical electric fields.

The azimuthal magnetic field above the ground illustrated in Fig. 27 remains unaffected by variations in the slope angle of the land-lake interface. Additionally, it is evident that the results obtained with the presence of the lake are identical to those without the lake (homogeneous ground). The electrical parameters of the propagation domain do not influence this component. Furthermore, in the presence of a stratified domain, the azimuthal magnetic field above the ground can be determined by utilizing the parameters of a single layer or by employing the perfectly conductive ground assumption.

Upon reviewing the preceding figures and observations, it is evident that the slope angle affects both components of the underground electric field, while only influencing the horizontal component above ground. This effect manifests itself as a reduction in the electric field's amplitude with increasing values of the angle θ, and conversely. With the high electrical parameters of the ocean, rendering it a conductive body, as the angle θ increases, the ocean covers more cells in the propagation medium, further intensifying its effect. The effect of the slope angle is slightly more pronounced in the land strike scenario than the CN Tower strike scenario. This difference is attributed to the higher electrical parameters assigned to the ocean than those used for the Lake.

4. CONCLUSION

In this paper, we have validated the staircase approach combined with Finite-Difference Time-Domain (FDTD) method for modeling geometries with slopes and analyzed its impact on lightning-induced electromagnetic fields. Two scenarios were studied:

✓ Land strike: The propagation domain consisted of land and ocean. Electromagnetic fields were simulated above and below the ground surface at two points: one located on land at a radial distance $r = 100\,\text{m}$ (with $dL = 1\,\text{m}$) and the other on the ocean at $r = 105\,\text{m}$.

✓ Lightning strike to the CN Tower (Toronto, Canada): A realistic geometry was modeled, including the land and Lake Ontario, to achieve high accuracy. Simulations were conducted above and below the ground at $r = 499\,\text{m}$ ($dL = 1\,\text{m}$).

The subsequent return stroke base current was modeled using the sum of two Heidler functions. For the land strike case, the current along the lightning channel followed the MTLE model, while for the CN Tower case, the current distribution was represented by the Baba and Rakov model. Maxwell's equations were solved using FDTD method, with staircase approach implemented to model land-ocean and land-lake interfaces.

Results demonstrated the effectiveness of the staircase approximation with FDTD in modeling geometries with slope angles.

In mixed land-ocean domains, the peak values of horizontal and vertical electric fields at underground observation points increased as the slope angle decreased. The azimuthal magnetic field was significantly affected by slope angles on ocean observation points, while its impact was less pronounced on land. Above ground, only the horizontal electric field component was sensitive to slope angles. While the land-lake interface exhibits similar behavior to the land-ocean case, the overall impact of the slope angle is smaller due to the lower conductivity of Lake Ontario. If the presence of the lake is neglected and the domain modeled as a single land layer, this simplification introduces noticeable errors in the predicted electromagnetic fields. This emphasizes the necessity of modeling the propagation domain as realistically as possible.

The FDTD method was confirmed as an efficient tool for modeling lightning electromagnetic fields due to its simplicity, versatility, and explicit time-domain formulation. The staircase approach employed in FDTD can be a good approximation for representing complex or curved structures, balancing accuracy and computational efficiency. FDTD's time-domain solutions make it ideal for transient phenomena like lightning. In contrast, Finite Element Method (FEM) is more computationally intensive and complex, requiring advanced expertise in meshing and solver configuration. The explicit nature of FDTD ensures faster and simpler implementation, making it a cornerstone method for solving Maxwell's equations across diverse electromagnetic applications.

Although staircase approximation provided sufficient accuracy for the large-scale scenarios considered in this study, future work could benefit from non-Cartesian or adaptive meshing techniques to more accurately represent complex terrain geometries, thereby reducing geometric approximation errors without significantly increasing computational cost.

REFERENCES

[1] Ghimire, B., S. Sharma, P. Karki, N. R. Karki, K. N. Poudyal, and C. Gomes, "Impact of a lightning strike on a low voltage transmission line: A case study from Fujel Gorkha, Nepal," in *2023 12th Asia-Pacific International Conference on Lightning (APL)*, 1–5, Langkawi, Malaysia, Jun. 2023.

[2] Matthee, A., P. W. Futter, R. Vogt-Ardatjew, and F. Leferink, "Lightning strike EMP effect on local grids," in *2021 Asia-Pacific International Symposium on Electromagnetic Compatibility (APEMC)*, 1–4, Nusa Dua-Bali, Indonesia, 2021.

[3] Junqua, I., F. Issac, D. Prost, T. Volpert, and A. Gaillot, "Methodology for the estimation of lightning effects on a nuclear reactor," *IEEE Transactions on Electromagnetic Compatibility*, Vol. 66, No. 1, 234–239, 2024.

[4] Huat, C. K., H. L. Cheun, A. K. K. Hing, L. K. Ten, S. Chia, and H. D. Sang, "Common mistakes in lightning protection design and installation," in *2023 12th Asia-Pacific International Conference on Lightning (APL)*, 1–6, Langkawi, Malaysia, Jun. 2023.

[5] Yee, K., "Numerical solution of initial boundary value problems involving Maxwell's equations in isotropic media," *IEEE Transactions on Antennas and Propagation*, Vol. 14, No. 3, 302–307, May 1966.

[6] Sarto, M. S., "Innovative absorbing-boundary conditions for the efficient FDTD analysis of lightning-interaction problems," *IEEE Transactions on Electromagnetic Compatibility*, Vol. 43, No. 3, 368–381, Aug. 2001.

[7] Tirkas, P. A., C. A. Balanis, M. P. Purchine, and G. C. Barber, "Finite-difference time-domain method for electromagnetic radiation, interference, and interaction with complex structures," *IEEE Transactions on Electromagnetic Compatibility*, Vol. 35, No. 2, 192–203, May 1993.

[8] Rakov, V. A. and F. Rachidi, "Overview of recent progress in lightning research and lightning protection," *IEEE Transactions on Electromagnetic Compatibility*, Vol. 51, No. 3, 428–442, Aug. 2009.

[9] Taflove, A. and K. R. Umashankar, "Review of FD-TD numerical modeling of electromagnetic wave scattering and radar cross section," *Proceedings of the IEEE*, Vol. 77, No. 5, 682–699, May 1989.

[10] Yang, C. and B. Zhou, "Calculation methods of electromagnetic fields very close to lightning," *IEEE Transactions on Electromagnetic Compatibility*, Vol. 46, No. 1, 133–141, Feb. 2004.

[11] Cooray, V., "Horizontal fields generated by return strokes," *Radio Science*, Vol. 27, No. 04, 529–537, Jul.-Aug. 1992.

[12] Rubinstein, M., "An approximate formula for the calculation of the horizontal electric field from lightning at close, intermediate, and long range," *IEEE Transactions on Electromagnetic Compatibility*, Vol. 38, No. 3, 531–535, Aug. 1996.

[13] Mimouni, A., F. Rachidi, and Z. Azzouz, "Electromagnetic environment in the immediate vicinity of a lightning return stroke," *Journal of Lightning Research*, Vol. 2, 64–75, 2007.

[14] Mimouni, A., F. Rachidi, and Z.-E. Azzouz, "A finite-difference time-domain approach for the evaluation of electromagnetic fields radiated by lightning strikes to tall structures," *Journal of Electrostatics*, Vol. 66, No. 9-10, 504–513, Sep. 2008.

[15] Schneider, J. B. and K. L. Shlager, "FDTD simulations of TEM horns and the implications for staircased representations," *IEEE Transactions on Antennas and Propagation*, Vol. 45, No. 12, 1830–1838, Dec. 1997.

[16] Dridi, K. H., J. S. Hesthaven, and A. Ditkowski, "Staircase-free finite-difference time-domain formulation for general materials

in complex geometries," *IEEE Transactions on Antennas and Propagation*, Vol. 49, No. 5, 749–756, May 2001.

[17] Lee, Y.-G., "Electric field discontinuity-considered effective-permittivities and integration-tensors for the three-dimensional finite-difference time-domain method," *Progress In Electromagnetics Research*, Vol. 118, 335–354, 2011.

[18] Cangellaris, A. C. and D. B. Wright, "Analysis of the numerical error caused by the stair-stepped approximation of a conducting boundary in fdtd simulations of electromagnetic phenomena," *IEEE Transactions on Antennas and Propagation*, Vol. 39, No. 10, 1518–1525, Oct. 1991.

[19] Holland, R., "Pitfalls of staircase meshing," *IEEE Transactions on Electromagnetic Compatibility*, Vol. 35, No. 4, 434–439, Nov. 1993.

[20] Akyurtlu, A., D. H. Werner, V. Veremey, D. J. Steich, and K. Aydin, "Staircasing errors in FDTD at an air-dielectric interface," *IEEE Microwave and Guided Wave Letters*, Vol. 9, No. 11, 444–446, Nov. 1999.

[21] Shoory, A., A. Mimouni, F. Rachidi, V. Cooray, and M. Rubinstein, "On the accuracy of approximate techniques for the evaluation of lightning electromagnetic fields along a mixed propagation path," *Radio Science*, Vol. 46, No. 02, 1–8, Apr. 2011.

[22] Wait, J. R., "Mixed path ground wave propagation: 1 short distances," *Journal of Research of the National Bureau of Standards*, Vol. 57, No. 1, 1–15, 1956.

[23] Paknahad, J., K. Sheshyekani, M. Hamzeh, D. Li, and F. Rachidi, "The influence of the slope angle of the ocean-land mixed propagation path on the lightning electromagnetic fields," *IEEE Transactions on Electromagnetic Compatibility*, Vol. 57, No. 5, 1086–1095, Oct. 2015.

[24] Li, Q., J. Wang, F. Rachidi, M. Rubinstein, A. Šunjerga, L. Cai, and M. Zhou, "Importance of taking into account the soil stratification in reproducing the late-time features of distant fields radiated by lightning," *IEEE Transactions on Electromagnetic Compatibility*, Vol. 61, No. 3, 935–944, 2019.

[25] Li, Q., M. Rubinstein, J. Wang, L. Cai, M. Zhou, Y. Fan, and F. Rachidi, "On the influence of the soil stratification and frequency-dependent parameters on lightning electromagnetic fields," *Electric Power Systems Research*, Vol. 178, 106047, Jan. 2020.

[26] Hou, W., M. Azadifar, M. Rubinstein, F. Rachidi, and Q. Zhang, "On the propagation of lightning-radiated electromagnetic fields across a mountain," *IEEE Transactions on Electromagnetic Compatibility*, Vol. 62, No. 5, 2137–2147, Oct. 2020.

[27] Mestriner, D. and M. Nicora, "On the importance of considering realistic orography into the evaluation of lightning electromagnetic fields in mixed path," *IEEE Transactions on Electromagnetic Compatibility*, Vol. 64, No. 5, 1442–1449, Oct. 2022.

[28] Jiang, L., X. Dong, X. Zhou, J. Wang, J. Song, and Q. Ma, "Propagation characteristics of lightning radiation field on three-layer vertical layered ground based on CPML absorption boundary," *IEEE Transactions on Electromagnetic Compatibility*, Vol. 65, No. 4, 1191–1201, Aug. 2023.

[29] Janischewskyj, W., A. M. Hussein, and V. Shostak, "Propagation of lightning current within the CN tower," *CIGRE Study Committee*, Vol. 33, 2–3, Canada, 1997.

[30] Heidler, F., J. Wiesinger, and W. Zischank, "Lightning currents measured at a telecommunication tower from 1992 to 1998," in *14th International Zurich Symposium and Technical Exposition on Electromagnetic Compatibility*, 1–6, Zurich, Zurich, Switzerland, Feb. 2001.

[31] Diendorfer, G., W. Hadrian, F. Hofbauer, M. Mair, and W. Schulz, "Evaluation of lightning location data employing measurements of direct strikes to a radio tower," *E & I Elektrotechnik Und Informationstechnik*, Vol. 119, No. 12, 422–427, 2002.

[32] Romero, C., F. Rachidi, M. Paolone, and M. Rubinstein, "Statistical distributions of lightning currents associated with upward negative flashes based on the data collected at the Säntis (EMC) tower in 2010 and 2011," *IEEE Transactions on Power Delivery*, Vol. 28, No. 3, 1804–1812, Jul. 2013.

[33] Rakov, V. A., "Transient response of a tall object to lightning," *IEEE Transactions on Electromagnetic Compatibility*, Vol. 43, No. 4, 654–661, Nov. 2001.

[34] Berger, K., "Parameters of lightning flashes," *Electra*, Vol. 80, 223–237, 1975.

[35] Koike, S., Y. Baba, T. Tsuboi, and V. A. Rakov, "Lightning current waveforms inferred from far-field waveforms for the case of strikes to tall objects," *IEEE Transactions on Electromagnetic Compatibility*, Vol. 65, No. 4, 1162–1169, Aug. 2023.

[36] Heidler, F. H. and C. Paul, "Field enhancement by lightning strikes to tall tower versus lightning strikes to flat ground," *IEEE Transactions on Electromagnetic Compatibility*, Vol. 63, No. 2, 550–557, Apr. 2021.

[37] Li, Z., Y. Ding, Y. Du, J. Cao, and M. Chen, "Integrated model for lightning strikes on a tall structure: Application to a wind turbine system," *IEEE Transactions on Electromagnetic Compatibility*, Vol. 65, No. 1, 271–280, Feb. 2023.

[38] Omari, M. and A. Mimouni, "Electromagnetic fields at very close range from a tower struck by lightning in presence of a horizontally stratified ground," *IEEE Transactions on Electromagnetic Compatibility*, Vol. 61, No. 1, 166–173, 2018.

[39] Omari, M. and A. Mimouni, "Electromagnetic fields at far distances from the peissenberg tower struck by lightning in presence of a horizontally stratified ground," in *2018 34th International Conference on Lightning Protection (ICLP)*, 1–7, Rzeszow, Poland, Sep. 2018.

[40] Mur, G., "Absorbing boundary conditions for the finite-difference approximation of the time-domain electromagnetic-field equations," *IEEE Transactions on Electromagnetic Compatibility*, Vol. 23, No. 4, 377–382, Nov. 1981.

[41] Heidler, F., "Analytic lightning current functions for LEMP calculations," in *18th International Conference on Lightning Protection (ICLP)*, Vol. 453, 63–66, VDE Verlag, Berlin, West Germany, 1985.

[42] Rachidi, F., W. Janischewskyj, A. M. Hussein, C. A. Nucci, S. Guerrieri, B. Kordi, and J.-S. Chang, "Current and electromagnetic field associated with lightning-return strokes to tall towers," *IEEE Transactions on Electromagnetic Compatibility*, Vol. 43, No. 3, 356–367, Aug. 2001.

[43] Nucci, C. A., C. Mazzetti, F. Rachidi, and M. Ianoz, "On lightning return stroke models for LEMP calculations," in *19th International Conference on Lightning Protection*, 463–469, 1988.

[44] Rachidi, F. and C. A. Nucci, "On the Master, Uman, Lin, Standler and the modified transmission line lightning return stroke current models," *Journal of Geophysical Research: Atmospheres*, Vol. 95, No. D12, 20 389–20 393, Nov. 1990.

[45] Versaci, M., F. Laganà, L. Manin, and G. Angiulli, "Soft computing and eddy currents to estimate and classify delaminations in biomedical device CFRP plates," *Journal of Electrical Engineering*, Vol. 76, No. 1, 72–79, 2025.

[46] Baba, Y. and V. A. Rakov, "Lightning electromagnetic environment in the presence of a tall grounded strike object," *Journal of Geophysical Research: Atmospheres*, Vol. 110, No. D9, D09108, May 2005.

[47] Rachidi, F., V. A. Rakov, C. A. Nucci, and J. L. Bermudez, "Effect of vertically extended strike object on the distribution of current along the lightning channel," *Journal of Geophysical Research: Atmospheres*, Vol. 107, No. D23, ACL 16–1–ACL 16–6, Dec. 2002.

[48] Mimouni, A., F. Rachidi, and Z.-E. Azzouz, "A finite-difference time-domain approach for the evaluation of electromagnetic fields radiated by lightning strikes to tall structures," *Journal of Electrostatics*, Vol. 66, No. 9–10, 504–513, Sep. 2008.

[49] Pavanello, D., F. Rachidi, W. Janischewskyj, M. Rubinstein, A. M. Hussein, E. Petrache, V. Shostak, I. Boev, C. A. Nucci, W. A. Chisholm, M. Nyffeler, J. S. Chang, and A. Jaquier, "On return stroke currents and remote electromagnetic fields associated with lightning strikes to tall structures: 2. Experiment and model validation," *Journal of Geophysical Research: Atmospheres*, Vol. 112, No. D13, Jul. 2007.

[50] Guerrieri, S., F. Heidler, C. A. Nucci, F. Rachidi, and M. Rubinstein, "Extension of two return stroke models to consider the influence of elevated strike objects on the lightning return stroke current and the radiated electromagnetic field: Comparison with experimental results," in *EMC'96 ROMA International Symposium on Electromagnetic Compatibility*, 701–706, Rome, Italy, Sep. 1996.